

# Mechanism of Qiguiyin Decoction Treats Pulmonary Infection Caused by *Pseudomonas aeruginosa* Based on Gut Microbiota and Metabolomics

Xuran Cui <sup>1-3</sup>, Xiaolong Xu<sup>1-3</sup>, Yahui Hu<sup>1,3</sup>, Rui Li<sup>1,3</sup>, Qingquan Liu<sup>1-3</sup>

<sup>1</sup>Beijing Hospital of Traditional Chinese Medicine, Capital Medical University, Beijing, 100010, People's Republic of China; <sup>2</sup>Beijing Institute of Chinese Medicine, Beijing, 100010, People's Republic of China; <sup>3</sup>Beijing Key Laboratory of Basic Research with Traditional Chinese Medicine on Infectious Diseases, Beijing, 100010, People's Republic of China

Correspondence: Qingquan Liu, Beijing Hospital of Traditional Chinese Medicine, Capital Medical University, Gallery Backstreet No.23, Dongcheng District, Beijing, 100010, People's Republic of China, Tel +8613910055687, Email liuqingquan\_2003@126.com

**Background:** Qiguiyin decoction (QGYD) was a traditional Chinese medicine (TCM) used to treat *Pseudomonas aeruginosa* infection in China. This study investigated the therapeutic effect and the potential mechanism of QGYD on carbapenem-resistant *Pseudomonas aeruginosa* (CRPA) infection.

**Materials and Methods:** Pulmonary infections were induced in mice by CRPA. The therapeutic effect of QGYD was evaluated by lung index and pulmonary pathology. The potential effects of QGYD on intestinal flora were detected by gut microbiome. The overall metabolism regulation of QGYD in blood was investigated by metabolomics. Next, the correlation between intestinal flora and metabolites was analyzed to illustrate the relationship between the regulatory effects of QGYD on metabolites and the beneficial effects of intestinal flora.

**Results:** QGYD has significant therapeutic effect on CRPA infection. QGYD profoundly inhibited the excessive accumulation of *Deferribacteres* and *Mucispirillum* at phylum and genus levels, respectively. Eleven potential metabolites that were abnormally expressed by CRPA infection and significantly reversed by QGYD were identified. Ten of the eleven metabolites significantly regulated by QGYD were related to *Deferribacteres*. *Deferribacteres* showed significant positive correlation with DL-lactic acid, phenylalanine and other metabolites and significant negative correlation with vitamin k1. At the genus level, *Mucispirillum* was closely related to metabolites significantly regulated by QGYD. *Mucispirillum* was positively correlated with metabolites such as DL-lactate and negatively correlated with vitamin k1.

**Conclusion:** QGYD can improve CRPA infection and has the effect of regulating intestinal flora and metabolism. It was a promising drug against infection.

**Keywords:** infection, drug-resistant bacteria, traditional Chinese medicine, Qiguiyin Decoction, pharmacodynamic mechanism

## Introduction

Carbapenem-resistant *Pseudomonas aeruginosa* (CRPA) poses a growing threat to global public health as it causes high morbidity and mortality. It has been classified by the World Health Organization (WHO) as a critical pathogen requiring urgent research and development of effective new antibiotic therapies.<sup>1,2</sup> Especially for multi-drug resistant CRPA, only a few drugs can inhibit it. These limited options make the treatment of infected patients very challenging, and the development of new antibacterial drugs has become a major problem that the medical community must address.<sup>3</sup>

Traditional Chinese medicine (TCM) is a valuable natural resource and a huge treasure trove in the drug discovery process.<sup>4</sup> Existing studies have proved that TCM can inhibit and kill bacteria. Meanwhile, they can also regulate the body's microecology and metabolism, and have definite curative effects and obvious advantages in the prevention and treatment of infectious diseases.<sup>5,6</sup> Qiguiyin decoction (QGYD) is a Chinese herbal compound developed according to many years of clinical experience in treating drug-resistant bacterial infection.<sup>7</sup> The prescription is composed of

*astragalus*, *angelica*, *Lonicera japonica* Thunb., *Reynoutria japonica* Houtt., *Artemisia annua* L., etc., and has remarkable efficacy in the treatment of PA infection. Previous studies exhibited that QGYD have the function of delay and reverse PA resistance to antibiotics, modulate inflammation and immune disorders, and enhance clinical curative effect against PA infection.<sup>8,9</sup> However, the pharmacodynamic mechanism of QGYD on CRPA infection remains unclear.

Studies have shown that the gut and lungs interact with each other when pulmonary infectious diseases occur. Respiratory pathogens, such as bacteria, lead to the disturbance of host symbiotic bacterial diversity, which may subsequently cause lung injury and affect intestinal function in host. Regulating intestinal flora to improve intestinal function helps to control lung infection and plays an important role in health recovery. In addition, the gut is considered to be an important target organ for regulating body functions due to its functions of immunity and nutrient uptake.<sup>10</sup> The intestinal microbiota directly regulates intestinal function, and the imbalance of intestinal microflora causes intestinal dysfunction, which directly influence the body's absorption and metabolism.<sup>11</sup> The combination of metabolomic and microbiome technologies shows that dysregulation of intestinal microbiome is directly related to the imbalance of multiple metabolites in many diseases.<sup>12</sup> The use of microbiome and metabolomics can help to reveal the mechanism of the drug.<sup>13</sup>

In this study, we select a carbapenem-resistant strain of multidrug-resistant *Pseudomonas aeruginosa* and investigated the efficacy of QGYD in the treatment of pulmonary infection caused by this strain in mice. It is worth mentioning that this strain is resistant to Imipenem, Ceftazidime-avibactam, Amikacin and sensitive to Levofloxacin, which are widely used in clinic. In addition, through microbiome and metabolomic techniques, the regulatory effect of QGYD on gut microecology and overall metabolism was explored, and the correlation between serum metabolites and gut microbes was analyzed to reveal the pharmacodynamic mechanism of QGYD.

## Materials and Methods

### Drugs

Preparation of the QGYD. QGYD consists of five herbs: *astragalus*, *angelica*, *Lonicera japonica* Thunb., *Reynoutria japonica* Houtt., *Artemisia annua* L.. All herbs were obtained from the Beijing Tong Ren Tang Group and mixed at a ratio of 12:3:3:2:2 (Beijing, China) with a total weight of 110g. After immersion for 1h, QGYD was obtained by water extraction twice. Next, the extract was filtered and condensed to 55 mL at a concentration of 2g herb/mL. Levofloxacin Tab. (LEV) was obtained from Daiichi Sankyo Pharmaceutical Co., Ltd. (Beijing, China). Imipenem and cilastatin sodium for injection (IPM) were bought from Merck sharp and Dohme Corp., U.S.A (Hangzhou, China).

### Animals and Strains

Four-week-old male BALB/c mice (specific pathogen free (SPF) were bought from Beijing Vital River Laboratory Animal Technology Co. Ltd (Beijing, China)). All the animals were kept in a controlled condition. The temperature was set at  $25 \pm 2^\circ\text{C}$ , the relative humidity was maintained at 45–60%, and the light/dark cycle was 12/12 hours. All animal experiments were conducted based on the approved guidelines of the Animal Care and Use Committee of the Beijing Institute of Chinese Medicine (BJTCM-M-2021-12-08). The CRPA strain (ATCC 3098) was provided by the Institute of Chinese Materia Medica, China Academy of Chinese Medical Sciences.

### Animal Experiment

The mouse infection model was set up based on the previous report with minor modifications.<sup>6</sup> Forty-eight BALB/c mice were randomly divided into control group (control), model group (model), LEV group (0.09 g/kg/d), IPM group (0.55 g/kg/d), QGYD high- and low-dose (QGYD H, 40.0 g/kg/d and QGYD L, 20 g/kg/d) group. Eight mice were included in each group. Mice in control, model, LEV, IPM and QGYD group were injected with 45  $\mu\text{L}$  ( $1 \times 10^{10}$  CFU/mL) CRPA suspension intranasally on the first day. The mice in control group were injected with 45  $\mu\text{L}$  normal saline. Mice in the QGYD group were orally given QGYD (0.2 mL/10g body weight) at the corresponding dose per day for 4 days, while mice in the LEV and IPM groups were given LEV and IPM, respectively. The mice in the control and model group were orally given distilled water. On the fifth day, the blood, lungs, and feces of the mice were collected for further analysis.

## Analysis of Lung Index

The lung tissues of mice were weighed, and the lung index was determined using the formula:

$$\text{lung index} = (\text{wet lung weight(g)}/\text{body weight(g)}) \times 100^{14}$$

## Examination of Histopathological

The left lung of mice was preserved in 4% paraformaldehyde. These tissues were mended after being fixed for at least 24 hours, dehydrated with gradient alcohol, and then embedded in paraffin. Next, the tissues were cut into 5  $\mu\text{m}$  slices and stained with hematoxylin and eosin.<sup>15</sup>

## Analysis on Gut Microbiome

Gut microbiome analysis was performed based on previous report with slight modification.<sup>16</sup> The hexadecyl trimethyl ammonium bromide (CTAB) method was adopted to extract total deoxyribonucleic acid (DNA) in feces samples. Next, the primers 341F: CCTACGGGNGGCWGCAG; 806R: GGACTACHVGGGTATCTAAT were used to amplify the V3-V4 domains of the 16S ribosomal RNA gene. In 1% agarose gels, the degree of DNA degradation, and the potential contamination was monitored. The purity of DNA (OD260/OD280, OD260/OD230) was determined by the Nanophotometer<sup>®</sup> spectrophotometer (IMPLEN, CA, USA). Qualified genomic DNA was firstly sonicated randomly, followed by end-repaired, A-tailed, and adaptor ligated based on the preparation regimen using NEBNext<sup>®</sup> MLtra<sup>™</sup> DNA Library Prep Kit for Illumina (NEB, USA). DNA fragments of 300 to 400 bp in length were amplified by PCR. Finally, AMPure XP system (Beckman Coulter, Brea, CA, USA) was used to purify the PCR products; and the size distribution of the library was analyzed using the 2100 Bioanalyzer (Agilent, Santa Clara, CA) and quantified by the real-time PCR. The pair-end technology (PE 150) was used to conduct the genome sequencing on an Illumina Novaseq 6000 sequencer.

The diversity and richness of intestinal microbial community were reflected by  $\alpha$  diversity. The microbial community composition was analyzed by  $\beta$  diversity. First, all the operational taxonomic unit (OTU) information of samples was stratified based on the minimum tags. Based on the species annotation results and OTU abundance information of all samples, the same kind of OTU information was combined to obtain the species abundance information analysis table. According to the unweighted\_unifrac method, the difference in the flora of control, model and QGYD group were analyzed by principal coordinate analysis (PCoA), species abundance histogram, and non-metric multidimensional scale (NMDS). The biomarkers among the groups were explored by the LEfSe (LDA effect size) method.

The clinical dose of QGYD was the low dose used in this study. Therefore, low dose of QGYD was used for analysis and study in microbiome and metabolome experiment, so as to provide basis for clinical research and application.

## Metabolomics Analysis

Metabolomics analysis was performed according to the previous description with slight modification.<sup>16</sup> First, equal amount of each extracted sample was obtained after all frozen serum samples were thawed. Next, the liquid chromatograph-mass spectrometer (LC-MS) was used to detect the samples. The analysis was conducted by an UHPLC (1290 Infinity LC, Agilent Technologies) coupled to a quadrupole time-of-flight (AB Sciex TripleTOF 6600). For HILIC separation, the 2.1 mm  $\times$  100 mm ACQUIY UPLC BEH 1.7  $\mu\text{m}$  column (waters, Ireland) was used to analyze samples. Finally, potential markers were identified in three groups. The screening criteria were those with the variable importance in the projection (VIP) value  $\geq 1.0$  and  $P$ -value  $\leq 0.05$ . The details of the detection of the metabolomics were described in the [Supplementary Material Metabolomics Analysis](#).

## Data Analysis

GraphPad Prism v.9 Software was used to analyze the data. Differences in data between two groups were analyzed by Student's  $t$ -test, and data among multiple groups were analyzed by one-way ANOVA. Data were expressed as mean  $\pm$  standard deviation (SD).  $P$ -value  $< 0.05$  meant that all data were statistically significant.<sup>15</sup>

## Results

### QGYD Inhibit the Increase of Lung Index in CRPA-Infected Mice and Had a Protective Effect on the Lung

First, the anti-infection effect of QGYD was determined by lung index. CRPA infection caused significant increase of lung index in mice ( $P < 0.0001$ ). QGYD ( $40.0$  and  $20.0 \text{ g} \cdot \text{kg}^{-1} \cdot \text{d}^{-1}$ ) significantly decreased the lung index and the effect of high dose was better than that of low dose ( $P < 0.001$ ,  $P < 0.01$ , [Figure 1a](#)).

The protective effect of QGYD on the lungs of CRPA-infected mice was evaluated by pulmonary pathology. The pulmonary characteristics of the mice in model group were severe widening of the alveolar septum, inflammatory cell infiltration, increased neutrophils and lymphocytes, local vasculitis, slight detachment of bronchial epithelial cells, and cell exudation in the lumen. By the intervention of QGYD ( $40.0$  and  $20.0 \text{ g} \cdot \text{kg}^{-1} \cdot \text{d}^{-1}$ ), the pathology induced by CRPA was improved, which was mainly reflected in the reduction of the degree of inflammatory cell infiltration and the inhibition of alveolar fusion. Meanwhile, pulmonary pathology was significantly improved in LEV group. Slight widening of alveolar septum and infiltration of inflammatory cells were the main pathological features. The pulmonary pathological structure of mice in IPM group was similar to that in model group ([Figure 1b](#)).

### Regulation of the Overall Structure of the Gut Microbiota

#### Gut Microbial Changes Among the Three Groups

16S rDNA sequencing was used to characterize changes in the composition of fecal microbiota after QGYD treatment. The Venn diagram ([Figure 2a](#)) showed 107, 113, 109 unique OTU in the control, model, QGYD group, respectively, and 248 common OTU among these groups. Sob, Shannon and Simpson indices were used to determine  $\alpha$ -diversity, and the differences among the three groups were not significant ([Figure S1a–f](#)). Next, the  $\beta$ -diversity was calculated by unweighted\_unifrac to estimate the overall microbial structure, and the result was visualized by the method of PCoA ([Figure 2b](#)) and NMDS ([Figure 2c](#)). Groups divided in this way were significantly different ([Figure 2d](#)). The distribution areas of samples in QGYD group and model group were obviously different, and the two groups had clear boundaries. There was only one sample crossed the control group. In summary, these results reveal that fecal contents were different among the groups.

#### Changes in Gut Microbes at the Phylum and Genus Levels

Next, the influence of QGYD on the composition of microbiota was explored. The top 10 phyla of the control, model, QGYD group were exhibited in [Figure 2e](#). The dominant bacteria in all three groups were *Bacteroidetes* and *Firmicutes*. Besides, the control group and the model group also included *Patescibacteria* and *Deferribacteres* as the dominant

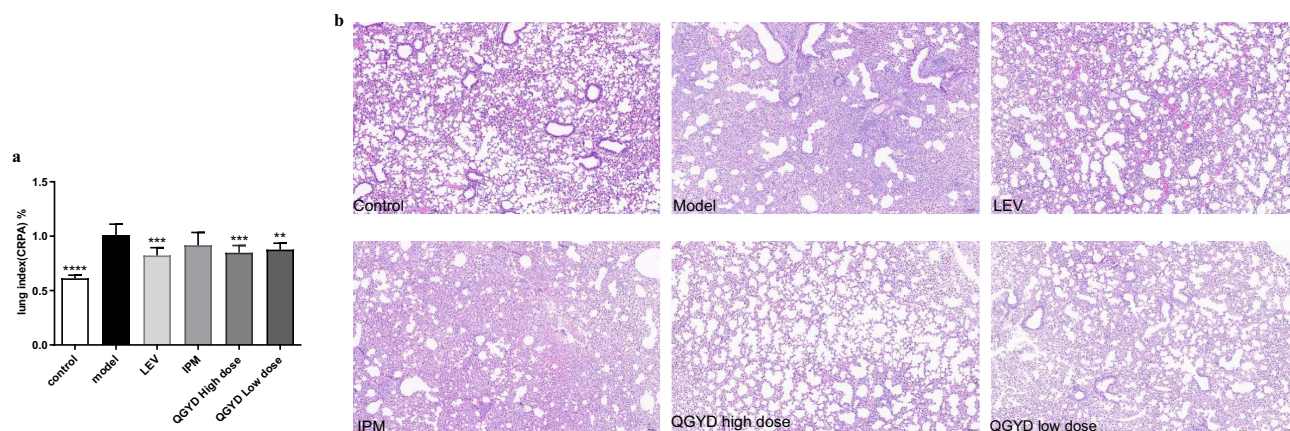


**Figure 1** Effect of QGYD on mice infected with CRPA. Mice were infected with CRPA intranasally. Six groups of mice were simultaneously treated orally with QGYD low- and high-dose ( $40$  and  $20 \text{ g} \cdot \text{kg}^{-1} \cdot \text{d}^{-1}$ ), LEV ( $0.09 \text{ g} \cdot \text{kg}^{-1} \cdot \text{d}^{-1}$ ), IPM ( $0.55 \text{ g} \cdot \text{kg}^{-1} \cdot \text{d}^{-1}$ ) or distilled water (control and model group) for 4 days. On day 5 after infection, the lungs of the mice were collected for lung index ([a](#)) and lung pathological analysis ([b](#)),  $\times 100$ ,  $n=4$ ). Result of lung index was expressed as mean  $\pm$ SD ( $n = 8$ ), and compared with the model group,  $**p < 0.01$ ,  $***p < 0.001$ ,  $****p < 0.0001$ .

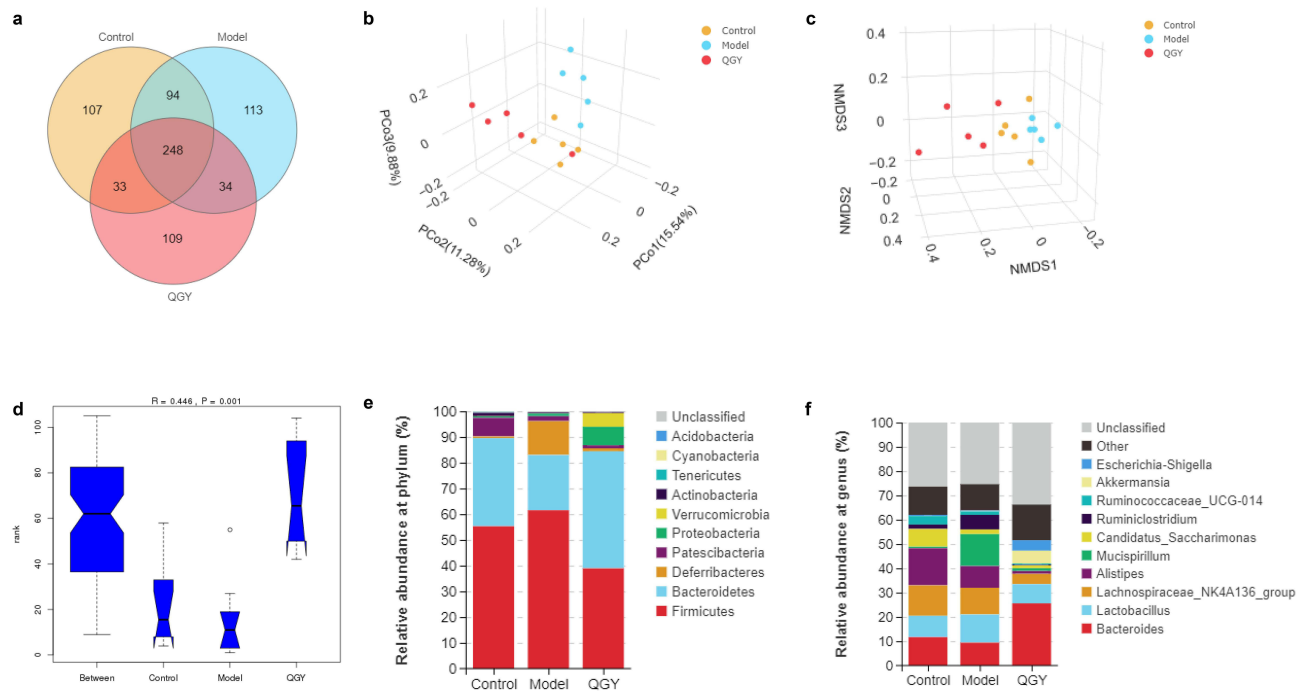


**Figure 2** Effects of QGYD on the overall structure of gut microbes. Mice were infected as described in Figure 1. (a) The Venn diagram showed the numbers of OTUs shared or not shared by 3 groups depending on overlaps. (b) PCoA analysis and (c) NMDS analysis. The axis of abscissa and the axis of ordinate represent the two selected main axes. Points of different colors or shapes represent samples of different groups. The closer the points of the two samples, the more similar the species composition of the two samples. (d) Rationality analysis of grouping. There were significant differences between the groups in the experiment. \*Means that one sample in the group was significantly different from the others. Column accumulation chart of relative abundance of species at phylum (e) and genus (f) level. The abscissa was grouping information, and the ordinate represented relative abundance. The sum of other species represented abundance less than 0.01 in the sample.

bacteria, respectively. The QGYD group also included *Proteobacteria* and *Verrucomicrobia*. Figure 2f shows the top 10 genera in control, model and QGYD group. The genera of bacteria were basically the same. *Bacteroides*, *Lactobacillus*, *Lachnospiraceae\_NK4A136\_group*, *Alistipes* and *Mucispirillum* were the most common bacteria. It was found that there were differences in microflora abundance among different groups (Tables S1 and S2).

At the genus level, *Lactobacillus*, *Mucispirillum* and *Ruminiclostridium* were among the bacteria with increased abundance and *Bacteroides*, *Lachnospiraceae\_NK4A136\_group*, *Ruminococcaceae\_UCG-014*, *Alistipes*, *Akkermansia*, *Candidatus\_Saccharimonas* and *Escherichia-Shigella* with a reduced abundance in the model group compared with the control group. Compared to the model group, bacteria with increased abundance in the QGYD group included *Bacteroides*, *Akkermansia* and *Escherichia-Shigella*, while the abundance of *Lactobacillus*, *Lachnospiraceae\_NK4A136\_group*, *Alistipes*, *Mucispirillum*, *Candidatus\_Saccharimonas*, *Ruminiclostridium* and *Ruminococcaceae\_UCG-014* were decreased.

### Effect of QGYD on Intestinal Flora Composition

Next, significant differences in microbial community abundance among the three groups were investigated (Figure 3a and b). It could be seen that *Deferribacteres* at phylum and *Mucispirillum* at genus in the model group were significantly increased compared with the control group ( $P < 0.001$ ). On the contrary, the abundance of these flora in QGYD group were adjusted markedly ( $P < 0.001$ ).

Then, the specific bacterial taxa of the three groups were examined using the method of the linear discriminant analysis effect size (LEfSe) (Figure 3c). Creatures with significant different gene abundance in each group can be obtained from the distribution histogram. The result showed that intestinal flora between groups had significant changes. In the control group, the dominant species were *Alistipes*, *Rikenellaceae*, *Ruminococcaceae\_UCG-014*, *Anaerofustis* and so on. In the model group, the dominant species were *Firmicutes*, *Clostridia*, *Deferribacteraceae*, *Mucispirillum*, *Ruminiclostridium* and so on. In the QGYD group, the dominant species were *Bacteroides*, *Rickettsia*, *Alteromonadales* and so on.

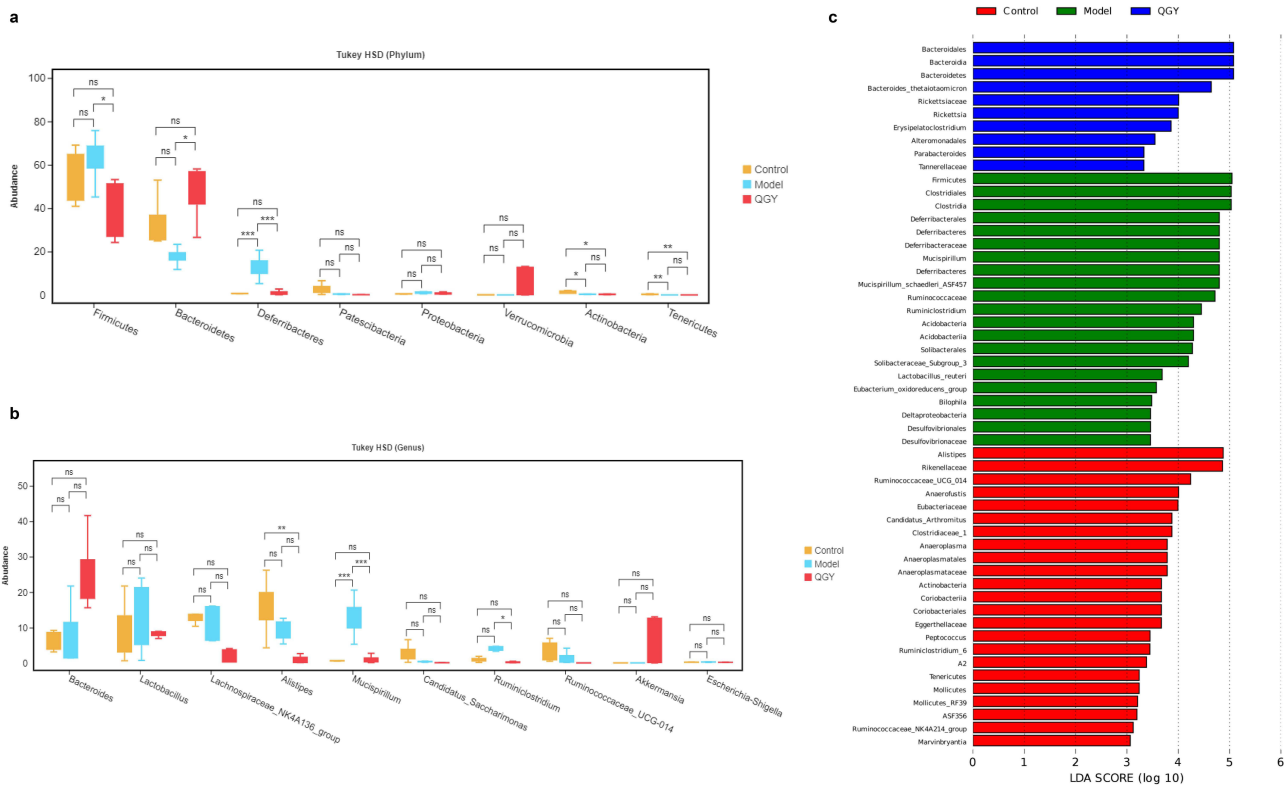


**Figure 3** Intestinal microbiological markers of QGYD against CRPA infection. Species annotation was completed on the representative sequences of OTUs, and the statistical analysis of the differences in community structure was performed based on the results of species annotations at phylum (a) and genus level (b). Compared with the model group, \* $P < 0.05$ , \*\* $P < 0.01$ , \*\*\* $P < 0.001$  indicates a significant difference. Ns indicates no significant difference between two groups. (c) LDA discriminant histogram. Count the microbial groups with significant effects in multiple groups and obtain the LDA score by LDA analysis (linear regression analysis). The larger the LDA score, the greater the impact of species.

Next, the experimental results of this part were comprehensively analyzed. After CRPA infection, the abundance of *Deferribacteres* in the model group increased significantly, ranking the third (Figures 2e and 3a) and being one of the characteristic floras at the phylum level (Figure 3c). Compared with the model group, the relative abundance of *Deferribacteres* was lower in the control and QGYD groups, and *Deferribacteres* was not included in the characteristic flora within the respective groups. At the genus level, *Mucispirillum* was one of the characteristic floras in the model group (Figure 3c) with a high relative abundance, ranking first (Figure 2f). Compared with the model group, the relative abundance of *Mucispirillum* was lower in the control group and QGYD group, showing a significant difference (Figure 3b). The results also showed some other characteristic flora in each group, but there was no statistical significance among the control, model and QGYD groups. For example, *Bacteroidetes* was the characteristic flora of the control group (Figure 3c), and the relative abundance of *Bacteroidetes* was the second in the control group (Figure 2e). Compared with the control group, the relative abundance of *Bacteroidetes* in the model group decreased but had no significant difference (Figure 3a). For another example, *Clostridia* and *Rickettsia* were the characteristic flora of the model group and the QGYD group, respectively. However, its abundance was relatively low (only the top 10 floras with high relative abundance were counted in the experiment).

## Metabolomic Study

### Changes in Metabolic

First, the metabolic changes based on LC-MS data under negative condition from serum samples were explored using the PLS-DA analysis. There was a good separation among these groups (Figure 4a), suggesting that CRPA infection caused changes in serum metabolites, and QGYD may be involved in regulating metabolic network abnormalities. Then, metabolites with significant changes were analyzed and identified. The samples of control group, model group and QGYD group showed

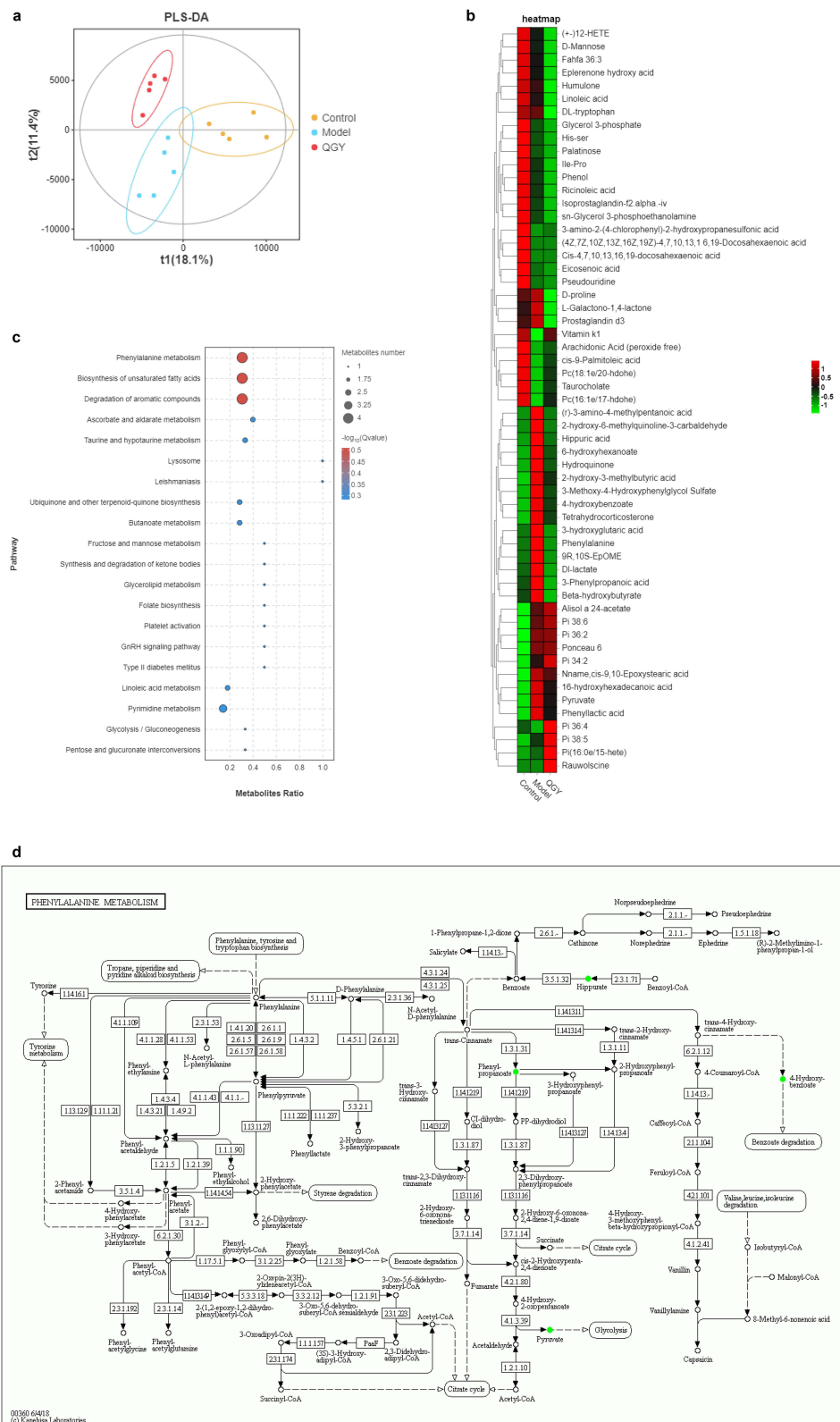


**Figure 4** Analysis of metabolic changes regulated by QGYD. (a) PLS-DA score charts. Samples from three different groups were represented by three different colors, and each group had five biological replicates. (b) Heat map for the differentially expressed metabolites. The relative content in the figure was displayed by the color difference, where the columns represented the sample, and the rows represented the metabolites. Each group had five biological replicates. At the bottom of the tree, each cluster extends a vertical line, after which it is aggregated by a horizontal line; each horizontal line was a category. The horizontal lines continue to aggregate from the bottom to the top. The more horizontal lines aggregate, the more concentrated the categories were. (c) Analysis of metabolic pathways of the control, model, and QGYD groups. Each dot represented a metabolic pathway, and there only marked top 20 metabolic pathways influenced by QGYD. (d) The detailed KEGG map of Phenylalanine metabolism pathways.

significant differences. Fifty-seven specific metabolic biomarkers were obtained by metabolome analysis to distinguish the Control vs Model vs QGYD. Hierarchical clustering analysis was then conducted for the 57 metabolites in each group (Figure 4b). The metabolites included Linoleic acid, Pyruvate, Pseudouridine, Phenyllactic acid, cis-9-Palmitoleic acid, etc. All metabolites were exhibited in Table S3. The color of each group in hierarchical clustering indicated the expression of corresponding metabolites. These data showed significant metabolomic differences among the groups. QGYD significantly recalled the level of some metabolites in the model group, among which the top 11 influential metabolites included DL-lactate, (r)-3-amino-4-methylpentanoic acid, Phenylalanine, 9R,10S-EpOME, 2-hydroxy-6-methylquinoline-3-carbaldehyde, 2-hydroxy-3-methylbutyric acid, L-Galactono-1,4-lactone, 4-hydroxybenzoate, 3-Phenylpropanoic acid, 3-hydroxyglutaric acid and Vitamin k1. For some other metabolites, QGYD only showed a correction trend, such as Hydroquinone, 6-hydroxyhexanoate and Pyruvate, or behaves in line with the model group, such as Cis-4,7,10,13,16,19-docosahexaenoic acid and 3-amino-2-(4-chlorophenyl)-2-hydroxypropanesulfonic acid.

Next, metaboAnalyst was conducted to make pathway analysis to gain a comprehensive understanding of these potential biomarkers and their functional roles. Based on the *p*-value or impact value, the top 20 metabolic pathways in three groups were analyzed (Figure 4c). Among them, there were four pathways with significant changes, namely, phenylalanine metabolism, biosynthesis of unsaturated fatty acids, degradation of aromatic compounds, ascorbate and aldarate metabolism. Detailed pathways for Control vs Model vs QGYD were presented in Table S4. In addition, the identified metabolites were mapped to the KEGG pathway database for in-depth interpretation of the individual functionals. The detailed KEGG map of Phenylalanine metabolism pathways among groups was taken as a typical example (Figure 4d).

### Correlation Analysis Between Gut Flora and Partial Metabolites

Finally, correlation analysis was performed on the three groups to more intuitively observe the relationship between metabolites and gut microbiota (Figure 5).

At phylum level, the flora closely associated with metabolites include *Deferribacteres*, *Patescibacteria*, *Bacteroidetes*, *Firmicutes* and so on. Ten of the eleven metabolites significantly regulated by QGYD were associated with *Deferribacteres*. *Deferribacteres* showed positive relationships with metabolites like DL-lactate, (r)-3-amino-4-methylpentanoic acid, Phenylalanine, 9R,10S-EpOME, 2-hydroxy-6-methylquinoline-3-carbaldehyde, 2-hydroxy-3-methylbutyric acid, 4-hydroxybenzoate, 3-Phenylpropanoic acid, 3-hydroxyglutaric acid and showed negative relationships with Vitamin k1. L-Galactono-

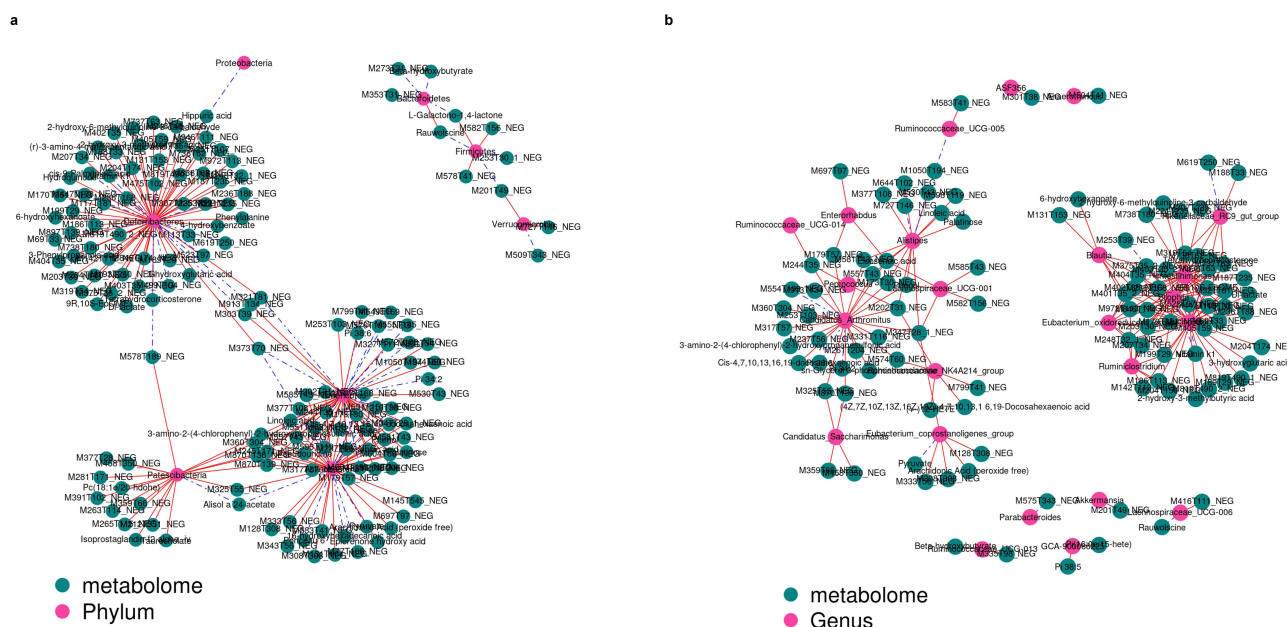


**Figure 5** Correlations of some metabolites with intestinal flora at phylum (a) and genus (b) levels. The solid red line and dashed blue line represented the positive and negative relationships between them. The absolute value of correlation coefficient between microorganisms and metabolites was greater than 0.5.

1,4-lactone and other metabolites significantly regulated by QGYD were positively correlated with *Firmicutes* but negatively correlated with *Bacteroidetes*. For some other metabolites, QGYD only showed a correction trend, such as Hydroquinone, 6-hydroxyhexanoate was also positively correlated with *Deferribacteres*. *Proteobacteria* was only negatively correlated with hippuric acid. 3-amino-2-(4-chlorophenyl)-2-hydroxypropanesulfonic acid, one of the metabolites that behaves in line with the model group, was positively correlated with *Actinobacteria* (Figure 5a).

At genus level, the flora closely associated with metabolites include *Mucispirillum*, *Candidatus\_Arthromitus*, *Intestinimonas*, *Ruminiclostridium* and so on. Among them, *Mucispirillum* was closely related to metabolites significantly regulated by QGYD. *Mucispirillum* was positively correlated with metabolites like DI-lactate, 2-hydroxy-3-methylbutyric acid, 9R,10S-EpOME, 3-hydroxyglutaric acid and showed negative relationships with Vitamin k1. 2-hydroxy-6-methylquinoline-3-carbaldehyde, DI-lactate showed positive relationships with *Intestinimonas*. 6-hydroxyhexanoate was also positively correlated with *Blautia*. 3-amino-2-(4-chlorophenyl)-2-hydroxypropanesulfonic acid was positively correlated with *Candidatus\_Arthromitus* (Figure 5b).

## Discussion

CRPA was an opportunistic pathogen that threatens human health seriously. It was easy to cause pulmonary infection.<sup>1</sup> In this experiment, mice were treated with CRPA strains to induce lung infection. Histological data showed that the lung structure of mice was significantly changed by CRPA, and the expression of inflammatory cells was the main characteristic. This was consistent with clinical findings.<sup>1</sup> The results further indicate that although QGYD can improve the lung structure of mice after CRPA infection, it does not restore it to normal status during the designed observation period. Under the same experimental conditions, LEV effectively improved the pulmonary pathological status of CRPA-infected mice, and the effectiveness levels of QGYD and LEV were similar. At the same time, the pulmonary pathological status in IPM group mice was not obviously improved, indicating that the treatment was ineffective. These data further confirm the resistance of CRPA strains and the effectiveness of QGYD in the treatment of pulmonary infection induced by drug-resistant bacteria.

More and more literatures have reported that bacterial lung infection is closely related to the composition and function of intestinal flora.<sup>17</sup> Bacteria cause lung injury and affect intestinal function in the host, while regulating intestinal flora helps to control lung infection.<sup>18</sup> Schuijt et al reported that fecal transplantation through oral gavage of normal intestinal flora restored the control of lung infection and the level of cytokines in the lung in mice, demonstrating the contribution of intestinal flora to lung immunity.<sup>19</sup> Therefore, it was of great significance to investigate the intestinal flora of the host during pulmonary infection, and it was an important way to explore the intervention effect and mechanism of therapeutic drugs. In this study, fecal samples were analyzed using 16S rDNA sequencing technology to determine changes in intestinal flora and analyze the regulatory effects of QGYD on intestinal flora. The taxonomic differences among the three groups were significant, indicating that CRPA had a strong interference effect on gut flora, and QGYD also has an obvious regulatory effect. *Bacteroidetes* and *Firmicutes* were the main microorganisms at phylum level. In addition, the control group and model group also included the dominant species *patescibacterium* and *Deferribacteres*, respectively. *Proteobacteria* and *Verrucomicrobia* were the dominant bacteria in QGYD group. Among them, only *Deferribacteres* showed significant changes in the three groups. CRPA infection leads to a significant increase in *Deferribacteres* abundance, which was significantly reduced by QGYD. At genus level, *Mucispirillum* abundance of the model group increased obviously, while the abundance of *Mucispirillum* in the QGYD group decreased markedly. Therefore, it is speculated that *Deferribacteres* and *Mucispirillum* were community markers at phylum and genus levels, respectively, and played the role of harmful pathogens in CRPA infection. *Mucispirillum* was the representative species of *Deferribacteres*. It has been reported that *Mucispirillum* inhibits the mucosal layer of the colon and may cause inflammation through mucin degradation.<sup>20</sup> The reduced mucus layer causes more luminal antigens to enter the immune system of the gut, leading to activation of the inflammatory response. For example, the accumulation of *Mucispirillum* bacteria could induce Crohn's disease-like colitis in Nod2/Cybb deficient mice. *Mucispirillum* specific immunoglobulin showed protective effect on intestinal tract of Nod2/Cybb deficient mice.<sup>20</sup> Therefore, it can be speculated that CRPA infection causes a large amount of accumulation of *Mucispirillum* in mice, and the increase of *Mucispirillum* may damage the intestinal mucosal layer of mice and stimulate inflammation, which may aggravate the degree of infection in

CRPA mice.<sup>21</sup> When QGYD was administered to intervene CRPA-infected mice under the same conditions, we observed a significant correction of *Mucispirillum* abundance, which was basically at the same level as that of control group. However, it has been reported that *Mucispirillum* does not return to normal levels until the convalescence period (after the pathogen has been cleared).<sup>20</sup> In this study, we speculated that QGYD might inhibit the excessive accumulation of *Mucispirillum* in mice at the early stage of CRPA infection, so as to avoid intestinal inflammation induced by *Mucispirillum* and thus inhibit the aggravation of infection. In addition, the control, model and QGYD group also contained other characteristic floras, respectively. For example, *Clostridia* and *Rickettsia* were respectively the characteristics of the model and QGYD group. The genus of *Clostridia* contains infectious pathogens such as *Clostridium*, which cause mild to severe gastrointestinal infections through the production of drug-resistant spores and toxin production.<sup>22</sup> *Rickettsia* was a Heritable microbe that may be related to typhus. However, there may be genetic symbiosis among animals without causing obvious disease.<sup>23</sup> The abundance of *Clostridia* and *Rickettsia* was relatively low, so it was speculated that they play a relatively negligible role in CRPA infection. Similarly, other flora with low relative abundance were not analyzed emphatically.

Intestinal flora has potential contribution to metabolic disorders.<sup>16</sup> More and more metabolomics has been studied in the regulation of metabolic disorders in various diseases.<sup>24–26</sup> It was of great significance to comprehensively understand the metabolome changes and the discovery of the potential biomarkers in mice infected with CRPA and the response for QGYD treatment. In this study, 11 potential metabolites that were abnormally expressed by CRPA infection and significantly reversed by QGYD were identified. It mainly includes DL-lactate, (r)-3-amino-4-methylpentanoic acid, Phenylalanine, 9R,10S-EpOME, 2-hydroxy-6-methylquinoline-3-carbaldehyde, L-Galactono-1,4-lactone, 4-hydroxybenzoate, 3-Phenylpropanoic acid, 2-hydroxy-3-methylbutyric acid, 3-hydroxyglutaric acid and Vitamin k1. These metabolites may be biomarkers of CRPA infection and were closely related to the pharmacodynamic effects of QGYD. DL-lactate, applied in food and other fields, greatly improves the safety, harmless to humans and animals, and has a strong bactericidal effect. In this study, the expression of DL-lactate in mice increased after infection, suggesting that the pathogen may stimulate the expression of DL-lactate in mice to resist the effect of the pathogen. DL-lactate in QGYD group was at the same level as that in control group, which may be because the infection of pathogens was inhibited in the early stage, and DL-lactate was maintained at the normal level without pathogen stimulation. In addition, phenylalanine was one of the essential amino acids of human body, which belongs to the aromatic amino acid.<sup>27</sup> Most of them were catalyzed and oxidized to tyrosine by phenylalanine hydroxylase in the body. Together with tyrosine, they synthesized important neurotransmitters and hormones involved in the body's metabolism of sugar and fat. The data of this experiment showed that the Phenylalanine expression in QGYD group was at the same level as that in control group, but the expression of Phenylalanine was lower compared with the model group. It suggests that CRPA infection affects the metabolic pathway of Phenylalanine and thus increases the degree of CRPA infection in mice. However, QGYD significantly improved this situation. Vitamin k1 was essential for the synthesis of prothrombin in the liver and can cause coagulation disorders when deficient.<sup>28</sup> When there is a lack of prothrombin in the blood, the coagulation of the blood will be delayed. The supplement of vitamin K1 could promote the liver synthesis of prothrombin and played the role of hemostasis.<sup>26</sup> From the results, the expression of vitamin K1 significantly decreased after CRPA infection, suggesting that it may cause coagulation disorder. However, QGYD significantly alleviated this unsatisfactory situation. Therefore, it was scientifically speculated that QGYD may have a function on CRPA infection by affecting the vitamin K1 expression to maintain the homeostasis of the blood in mice.

Next, we analyzed the correlation between intestinal flora and metabolites to illustrate the relationship between the regulatory effects of QGYD on metabolites and the beneficial effects of intestinal flora. The results showed that 10 of the 11 metabolites significantly regulated by QGYD were related to *Deferribacteres* at the phylum level. There was a positive correlation between *Deferribacteres* and DL-lactate, phenylalanine, and other metabolites, but a negative correlation between *Deferribacteres* and vitamin k1. At the genus level, *Mucispirillum* was closely related to metabolites significantly regulated by QGYD. *Mucispirillum* was positively correlated with metabolites such as DL-lactate and negatively correlated with vitamin k1. It was further suggested that 11 metabolites significantly regulated by QGYD may be the key metabolites in the treatment of CRPA infection. It was also suggested that the change of metabolite expression is related to the change of intestinal flora.

Based on this study, we speculated that CRPA infection caused changes in the intestinal flora of mice, and subsequently affected the normal expression of various metabolites, thus aggravating the degree of infection. However, the intervention of QGYD effectively ameliorates this condition, which may be an important way for its effectiveness. The role of QGYD on the regulation of gut flora and metabolism of the mice only proves its possible effect on the treatment of CRPA infection, which provides biological basis for the theory of treating different diseases with the same treatment in traditional Chinese medicine. This study explored significant differences and biomedical characteristics among the three groups of mice, but considering the limited number of mice, the followed work will increase the sample size for in-depth investigation of the effect and mechanism of QGYD in CRPA infection.

## Conclusion

Mice infected with CRPA had obvious changes in lung pathological structure, extensive changes in gut microbiota and metabolome profile. QGYD could alleviate the severity of pulmonary infection in mice, regulate the disorder of intestinal flora, partially reverse the abnormal metabolome, and thus improve the infection. In addition, metabolites significantly regulated by QGYD, such as D-lactate and Vitamin K1, were closely related to *Deferribacteres* and *Mucispirillum*. However, given the limited number of mice in this experiment, future work will increase the number of samples to further investigate the effect and mechanism of QGYD on CRPA infection.

## Abbreviations

CRPA, carbapenem-resistant *Pseudomonas aeruginosa*; CTAB, hexadecyl trimethyl ammonium bromide; NMDS, non-metric multidimensional scale; OTU, operational taxonomic units; PCoA, principal coordinate analysis; QGYD, Qiguiyin decoction; SPF, specific pathogen free; SD, standard deviation; TCM, traditional Chinese medicine.

## Acknowledgments

This work was supported by grants from the National Traditional Chinese Medicine Multidisciplinary Innovation Team Project (ZYYCXTD-D-202201) and Natural Science Foundation of Capital Medical University (PYZ22166).

## Disclosure

Professor Qingquan Liu reports a patent A new use of Chinese medicine licensed to CN102379931B. The authors report no other conflicts of interest in this work.

## References

1. Murray CJL, Ikuta KS, Sharara F; Antimicrobial Resistance Collaborators. Global burden of bacterial antimicrobial resistance in 2019: a systematic analysis. *Lancet*. 2022;399:629–655. doi:10.1016/S0140-6736(21)02724-0
2. Evelina T, Elena C, Alessia S, et al. Discovery, research, and development of new antibiotics: the WHO priority list of antibiotic-resistant bacteria and tuberculosis. *Lancet Infect Dis*. 2018;18:318–327. doi:10.1016/S1473-3099(17)30753-3
3. Matteo B, Garyphallia P, Etienne R, et al. Antimicrobial resistance in the next 30 years, humankind, bugs and drugs: a visionary approach. *Intensive Care Med*. 2017;43:1464–1475. doi:10.1007/s00134-017-4878-x
4. Shengyan X, Yunhong L, Lifeng Y, et al. Role of traditional Chinese medicine in the management of viral pneumonia. *Front Pharmacol*. 2020;11:582322. doi:10.3389/fphar.2020.582322
5. Zheng P, Qingjun Z. Traditional Chinese medicine is an alternative therapeutic option for treatment of *Pseudomonas aeruginosa* infections. *Front Pharmacol*. 2021;12:737252. doi:10.3389/fphar.2021.737252
6. Hou Y, Nie Y, Cheng B, et al. Qingfei Xiaoyan Wan, a traditional Chinese medicine formula, ameliorates *Pseudomonas aeruginosa*-induced acute lung inflammation by regulation of PI3K/AKT and Ras/MAPK pathways. *Acta Pharm Sin B*. 2016;6(3):212–221. doi:10.1016/j.apsb.2016.03.002
7. Po H, Yuhong G, Jingxia Z, et al. "Efficacy and safety of the Qiguiyin formula in severe pneumonia: study protocol for a randomized, double-blind, placebo-controlled clinical trial". *J Tradit Chin Med*. 2020;40:317–323.
8. Guochao C, Wanqiao Z, Lingbo K, et al. Qiguiyin decoction improves multidrug-resistant *Pseudomonas aeruginosa* infection in rats by regulating inflammatory cytokines and the TLR4/MyD88/NF- $\kappa$ B signaling pathway. *Biomed Res Int*. 2022;2022:5066434. doi:10.1155/2022/5066434
9. Ling-Bo K, Qun M, Jie G, et al. Effect of Qiguiyin decoction on multidrug-resistant *Pseudomonas aeruginosa* infection in rats. *Chin J Integr Med*. 2015;21:916–921. doi:10.1007/s11655-015-2089-2
10. Seon-Kyun K, Guevarra Robin B, You-Tae K, et al. Role of probiotics in human gut microbiome-associated diseases. *J Microbiol Biotechnol*. 2019;29:1335–1340. doi:10.4014/jmb.1906.06064
11. Yong F, Oluf P. Gut microbiota in human metabolic health and disease. *Nat Rev Microbiol*. 2021;19:55–71. doi:10.1038/s41579-020-0433-9
12. Yue S, Sheng-Di W, Yao C, et al. Alterations in gut microbiome and metabolomics in chronic hepatitis B infection-associated liver disease and their impact on peripheral immune response. *Gut Microbes*. 2023;15:2155018. doi:10.1080/19490976.2022.2155018

13. Wenya J, Yaxin S, Xianghong W, et al. Metabonomics and the gut microbiome analysis of the effect of 6-shogaol on improving obesity. *Food Chem.* 2023;404:134734. doi:10.1016/j.foodchem.2022.134734
14. Zhang T, Xiao M, Wong C-K. Sheng Jiang San, a traditional multi-herb formulation, exerts anti-influenza effects in vitro and in vivo via neuraminidase inhibition and immune regulation. *BMC Complement Altern Med.* 2018;18:150. doi:10.1186/s12906-018-2216-7
15. Xu-Ran C, Yu-Hong G, Qing-Quan L. Cangma Huadu granules, a new drug with great potential to treat coronavirus and influenza infections, exert its efficacy through anti-inflammatory and immune regulation. *J Ethnopharmacol.* 2022;287:114965. doi:10.1016/j.jep.2021.114965
16. Piao S, Zhu Z, Tan S, et al. An integrated fecal microbiome and metabolome in the aged mice reveal anti-aging effects from the intestines and biochemical mechanism of FuFang zhenshu TiaoZhi (FTZ). *Biomed Pharmacother.* 2020;121:109421. doi:10.1016/j.biopha.2019.109421
17. Rafail M, Anna N, Efthimia P, et al. Gut microbiota modulation and prevention of dysbiosis as an alternative approach to antimicrobial resistance: a narrative review. *Yale J Biol Med.* 2022;95:479–494. doi:10.1101/gr.096651.109
18. Adriana NM, Damiana-Maria V, Diana G, et al. Gastrointestinal microbiota: a predictor of COVID-19 severity? *World J Gastroenterol.* 2022;28:6328–6344. doi:10.3748/wjg.v28.i45.6328
19. Schuijt TJ, Lankelma JM, Scicluna BP, et al. The gut microbiota plays a protective role in the host defence against pneumococcal pneumonia. *Gut.* 2015;65:575–583.
20. Caruso R, Mathes T, Martens EC, et al. A specific gene-microbe interaction drives the development of Crohn's disease-like colitis in mice. *Sci Immunol.* 2019;4:undefined. doi:10.1126/sciimmunol.aaw4341
21. Wolff Nora S, Jacobs Max C, Joost WW, et al. Pulmonary and intestinal microbiota dynamics during Gram-negative pneumonia-derived sepsis. *Intensive Care Med Exp.* 2021;9:35. doi:10.1186/s40635-021-00398-4
22. Soroush B, Sepide K, Shirin D, et al. Global prevalence of *Clostridioides difficile* in 17,148 food samples from 2009 to 2019: a systematic review and meta-analysis. *J Health Popul Nutr.* 2023;42:36. doi:10.1186/s41043-023-00369-3
23. Panupong T, Davison Helen R, Thompson David J, et al. Incidence and diversity of torix Rickettsia-Odonata symbioses. *Microb Ecol.* 2021;81:203–212. doi:10.1007/s00248-020-01568-9
24. Congcong C, Junshen T, Xiaoxia G, et al. An integrated strategy to study the combination mechanisms of *Bupleurum chinense* DC and *Paeonia lactiflora* Pall for treating depression based on correlation analysis between serum chemical components profiles and endogenous metabolites profiles. *J Ethnopharmacol.* 2022;305:116068. doi:10.1016/j.jep.2022.116068
25. Jian F, Xia G, Xialin C, et al. Mechanism of Jinzhen Oral Liquid against influenza-induced lung injury based on metabonomics and gut microbiome. *J Ethnopharmacol.* 2023;303:115977. doi:10.1016/j.jep.2022.115977
26. Maik K, Loes M, van der Peet M, et al. Unraveling antimicrobial resistance using metabolomics. *Drug Discov Today.* 2022;27:1774–1783. doi:10.1016/j.drudis.2022.03.015
27. Galles Grace D, Infield Daniel T, Clark Colin J, et al. Tuning phenylalanine fluorination to assess aromatic contributions to protein function and stability in cells. *Nat Commun.* 2023;14:59. doi:10.1038/s41467-022-35761-w
28. Heng Z, Mei L, Xue-Lian A, et al. Randomized, placebo-controlled trial of orally administered vitamin K1 for warfarin-associated coagulopathy in Chinese patients with mechanical heart valves. *Eur J Clin Pharmacol.* 2021;77:1333–1339. doi:10.1007/s00228-021-03127-8

## Infection and Drug Resistance

Dovepress

### Publish your work in this journal

Infection and Drug Resistance is an international, peer-reviewed open-access journal that focuses on the optimal treatment of infection (bacterial, fungal and viral) and the development and institution of preventive strategies to minimize the development and spread of resistance. The journal is specifically concerned with the epidemiology of antibiotic resistance and the mechanisms of resistance development and diffusion in both hospitals and the community. The manuscript management system is completely online and includes a very quick and fair peer-review system, which is all easy to use. Visit <http://www.dovepress.com/testimonials.php> to read real quotes from published authors.

Submit your manuscript here: <https://www.dovepress.com/infection-and-drug-resistance-journal>